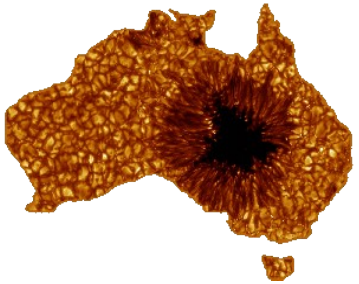

SOHO 19/GONG 2007, 9-13 July 2007

Time-Distance Helioseismology of Sunspots

examples of contamination by surface effects

Sébastien Couvidat
HEPL, Stanford University

Time-Distance Helioseismology

- Phase-speed filtering of the Doppler velocity datacube (Duvall et al. 1997)
- Computing the point-to-point cross-covariances between source ($\mathbf{r}_1$) and receiver ($\mathbf{r}_2$)
- Different averaging schemes depending on the physical effect we are interested in [sound speed c(z), flow velocity $\mathbf{v}(\mathbf{r},z)$]

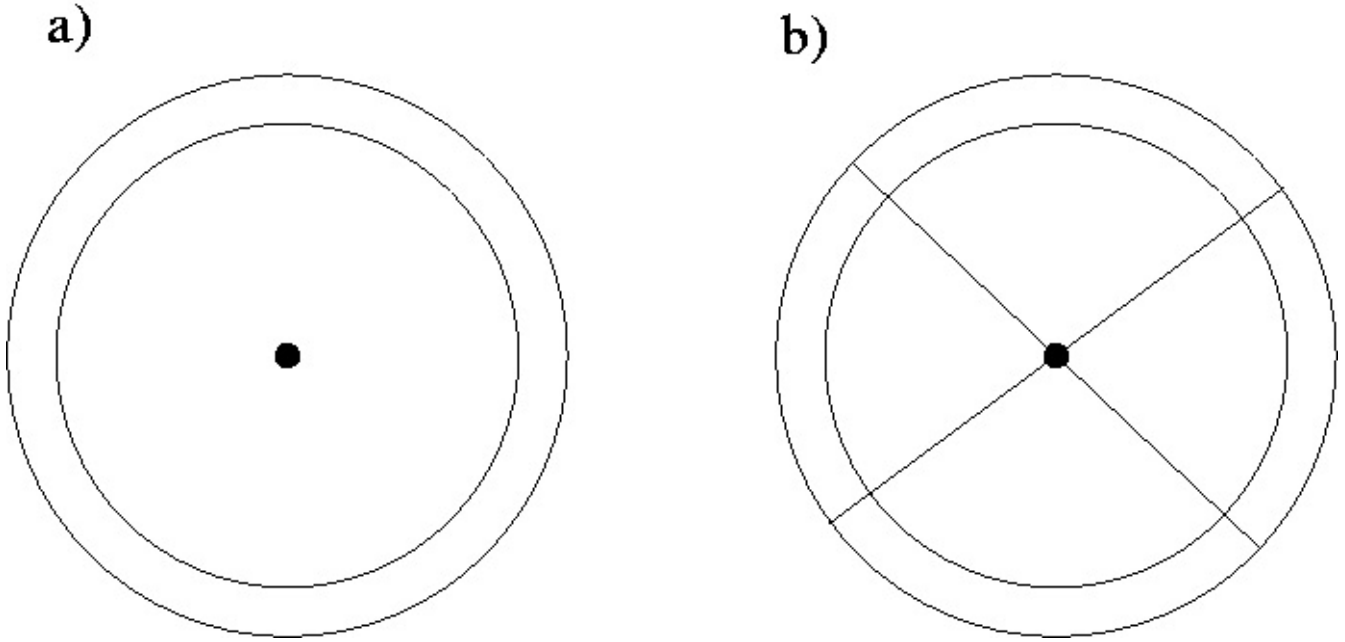

a) center-to-annulus averaging
b) east-west and north-south quadrant averaging

- Ingoing and outgoing travel time are fitted by Gabor wavelet (Kosovichev & Duvall 1997)

Inversion Algorithm

- We invert integral relations relating: i) mean travel-time perturbations to sound-speed perturbations ii) difference travel-time perturbations to flow velocities
- Based on MCD (Jensen, Jacobsen, & Christensen-Dalsgaard 1998)
- modified to include (Couvidat et al. 2005):
  - horizontal regularization
  - cross-covariance matrix of the noise on the travel-time maps (based on noise model by Gizon & Birch 2004)
- Uses 3 kinds of kernels:
    - Ray-approximation kernels (e.g. Giles 1999; Kosovichev, Duvall, & Scherrer 2000)
    - Fresnel-zone/Rytov-approximation kernels (Jensen & Pijpers 2003)
    - Born-approximation kernels (Birch, Kosovichev, & Duvall 2004)

Sound-speed structure with Fresnel-zone kernels

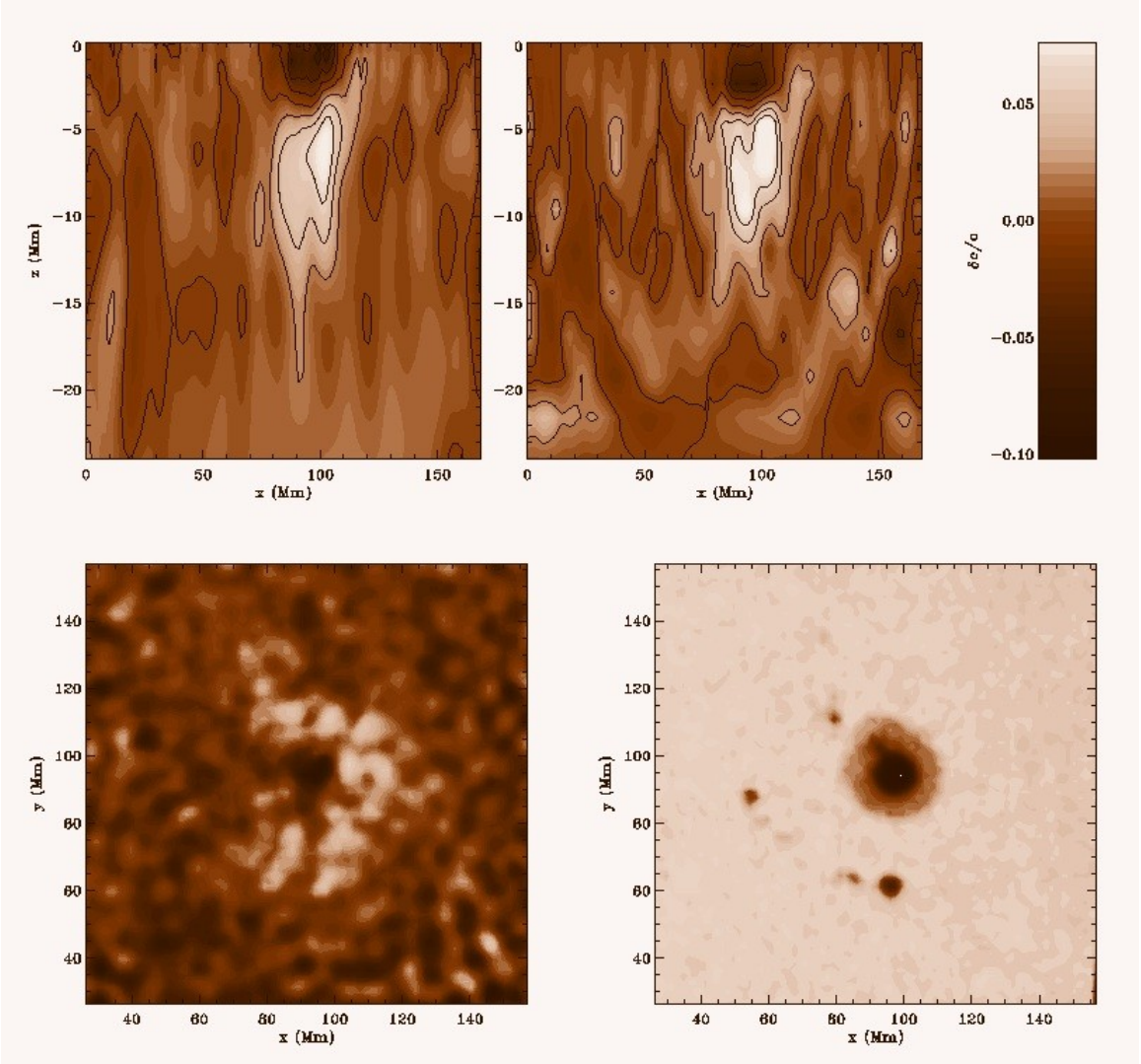

Inversion of AR 8243 (June 1998) with Fresnel-zone (upper left and lower left panels) and ray-path (upper right panel) kernels. Upper panels: vertical cut of the inversion results. Lower right panel: continuum intensity at the solar surface. Lower left panel: cut in the horizontal plane at a depth of 3.3 Mm. Below the main sunspot, two finger-like structures are visible, that seem to connect the two pores visible on the lower right panel at 35 Mm from the center of the spot.

From Couvidat, Birch, Kosovichev, & Zhao (2004)

Sound-speed structure with Born-approximation kernels

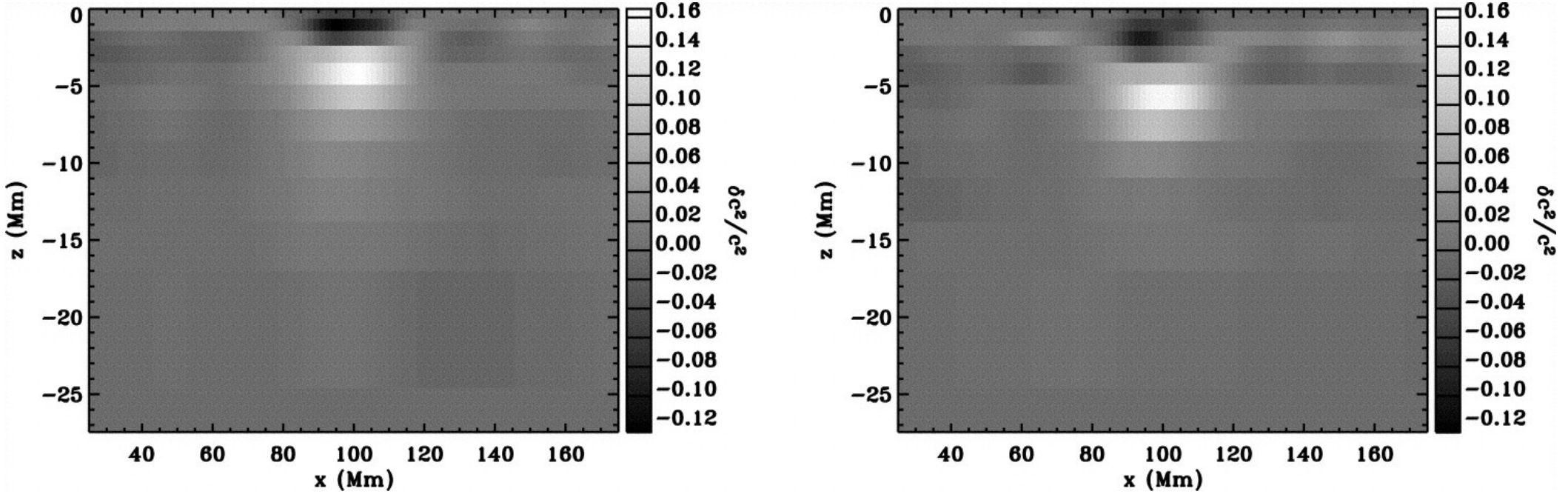

Vertical cut in the inversion results around y = 97 Mm. Left: Inversion using Born approximation kernels. Right: Inversion using ray-path kernels.

From Couvidat, Birch, & Kosovichev (2006)

Possible contamination by surface magnetic field: ring-like structures

· Produced datacubes for 16 sunspots (between 1997 and 2006), with MDI Hi-Res data
· Datacubes: 256 x 256 x 512 nodes, dx=dy=0.826 Mm, dt=1 min
· Compute the mean and difference travel-time maps for these sunspots for 11 distances source-receiver
· Inverted the travel times using Born approximation kernels (provided by A. C. Birch), and modified MCD algorithm

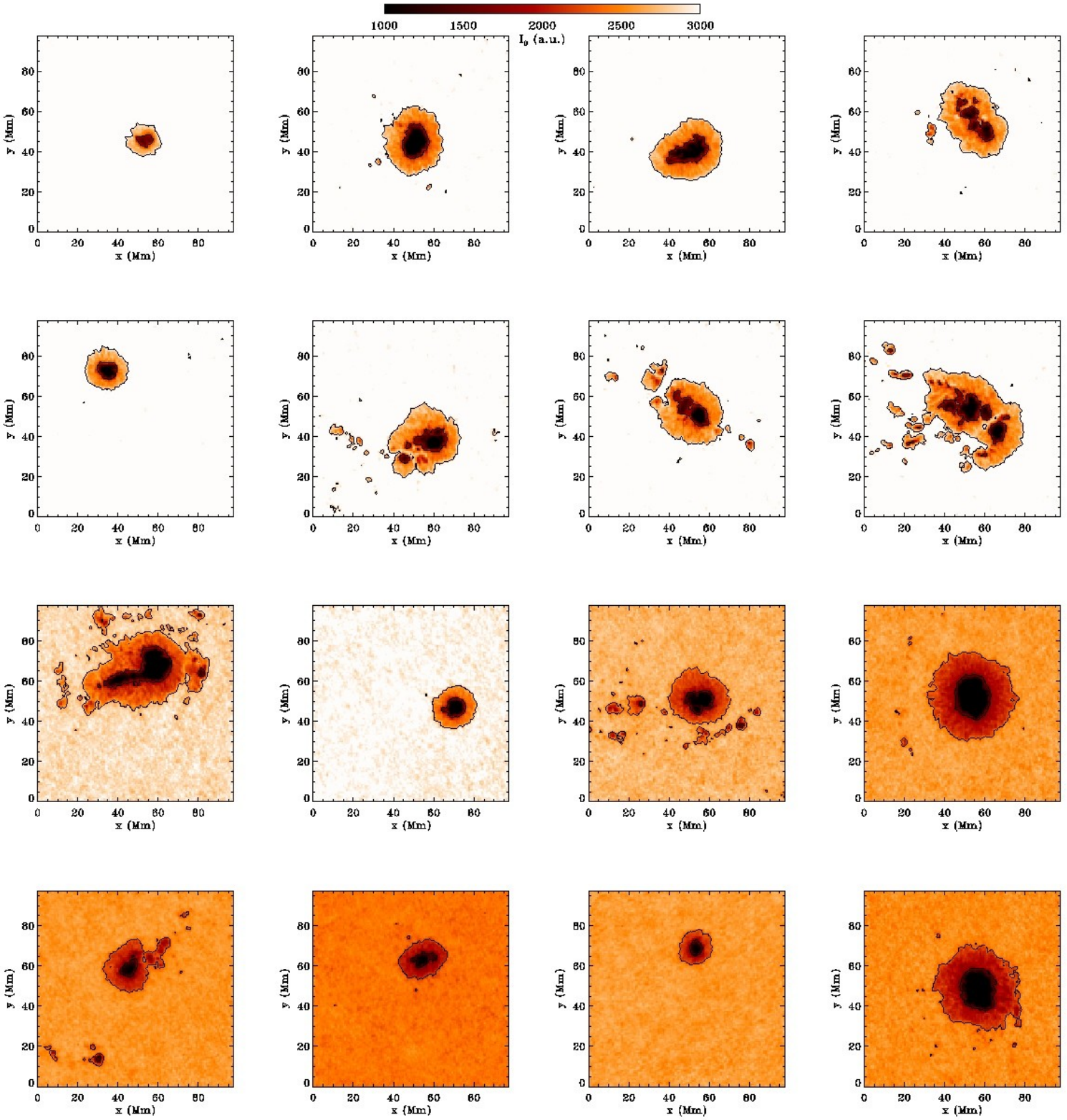

Continuum intensity maps of 16 solar active regions (From Couvidat & Rajaguru 2007)

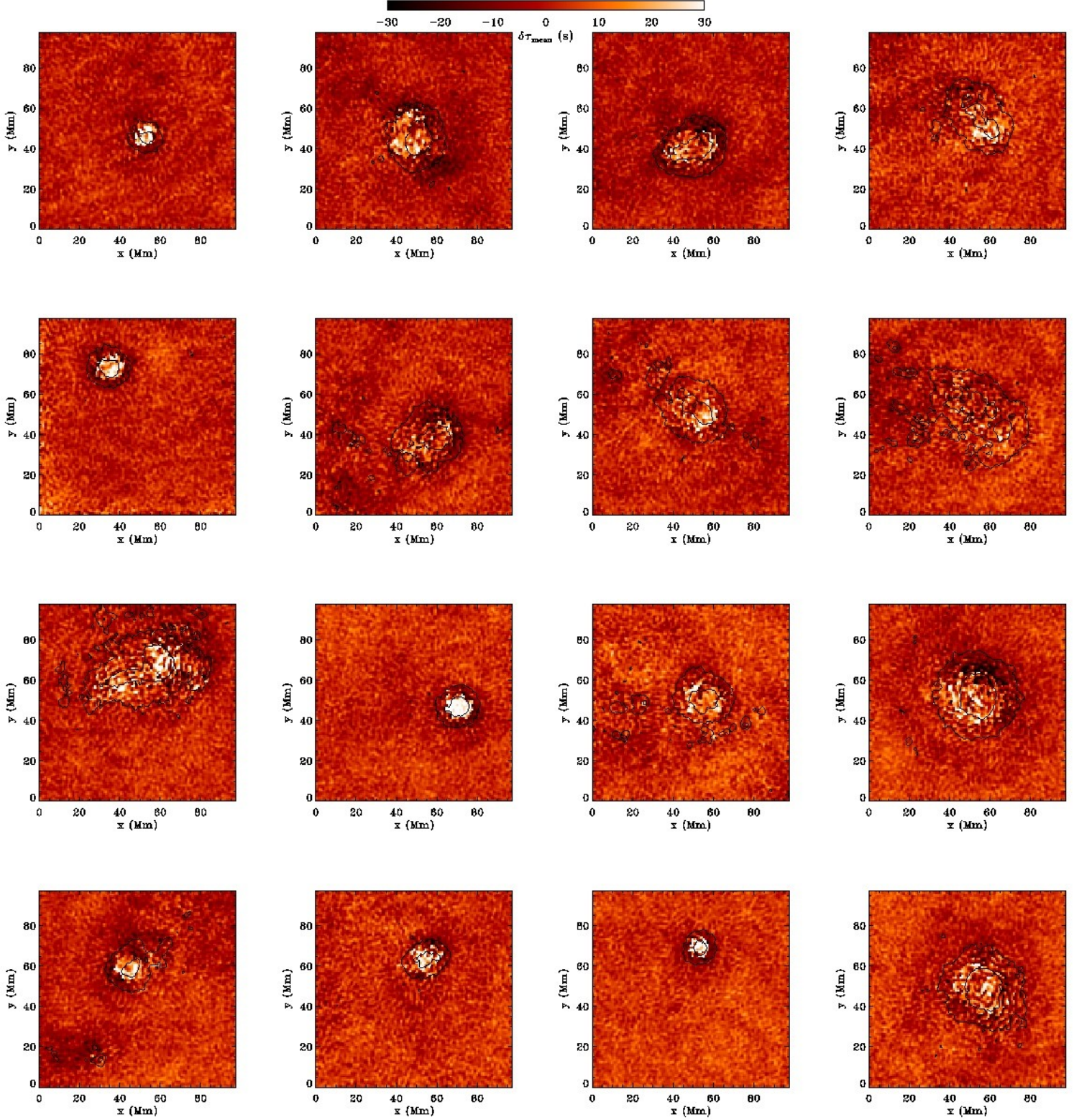

Mean travel-time perturbation maps at 11.6 Mm

(From Couvidat & Rajaguru 2007)

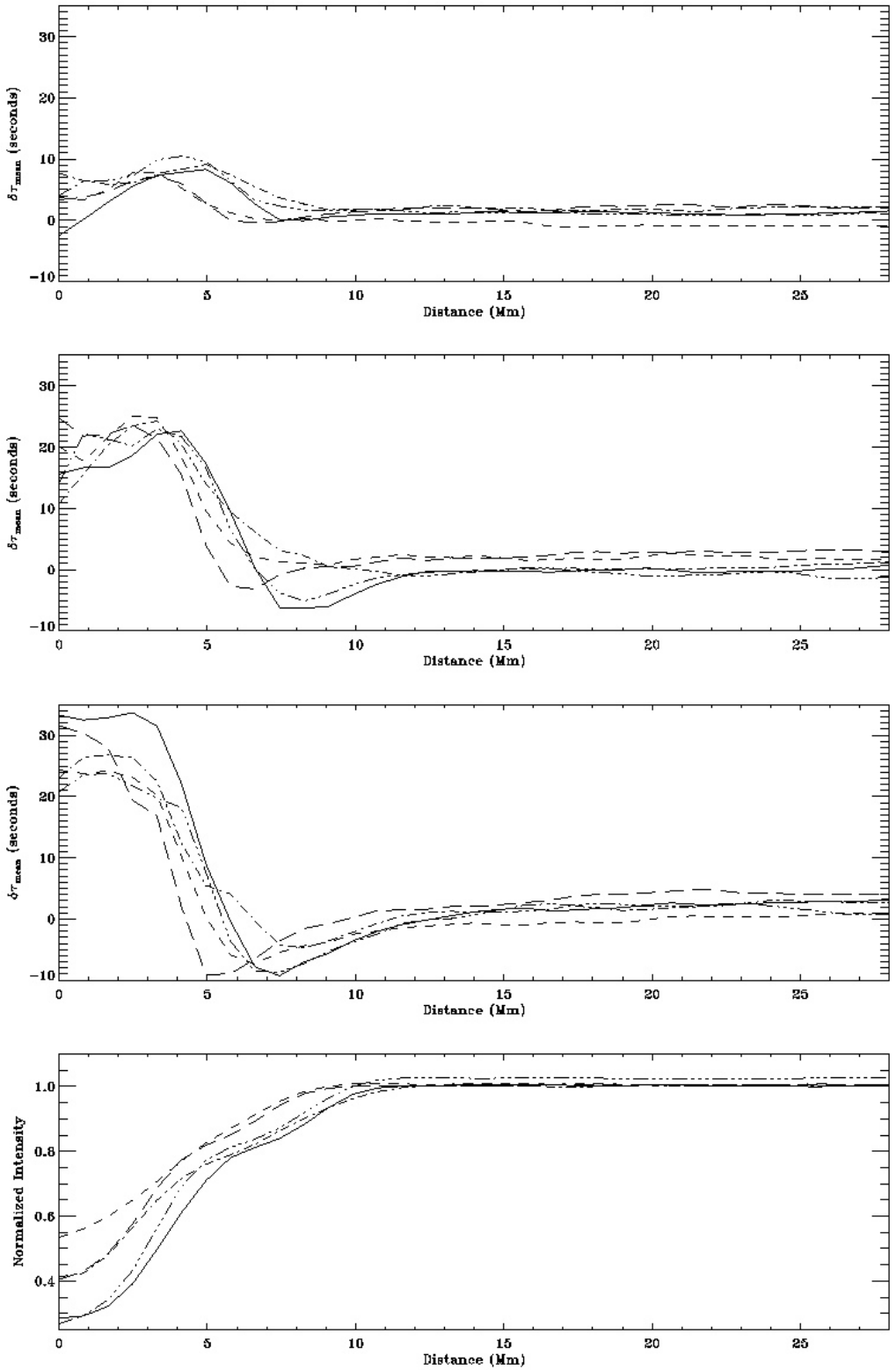

Azimuthal average of the mean travel-time perturbation for 5 circular sunspots, around the spot center at 6.2 Mm (upper panel), 8.6 Mm (middle), and 11.6 Mm (lower)

(From Couvidat & Rajaguru 2007)

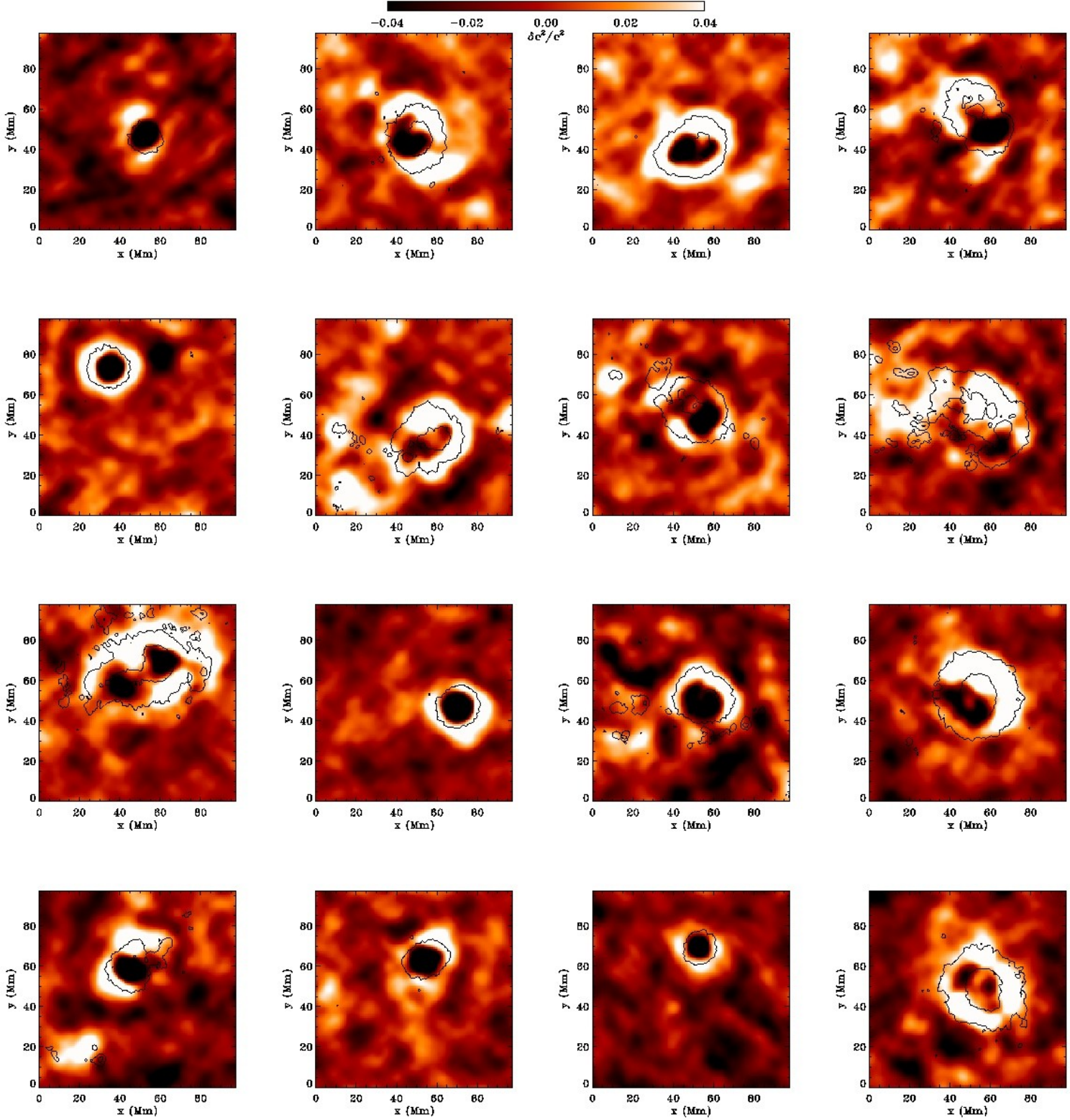

Relative sound-speed perturbation at a depth of z=-2.38 to z=-1.42 Mm

(From Couvidat & Rajaguru 2007)

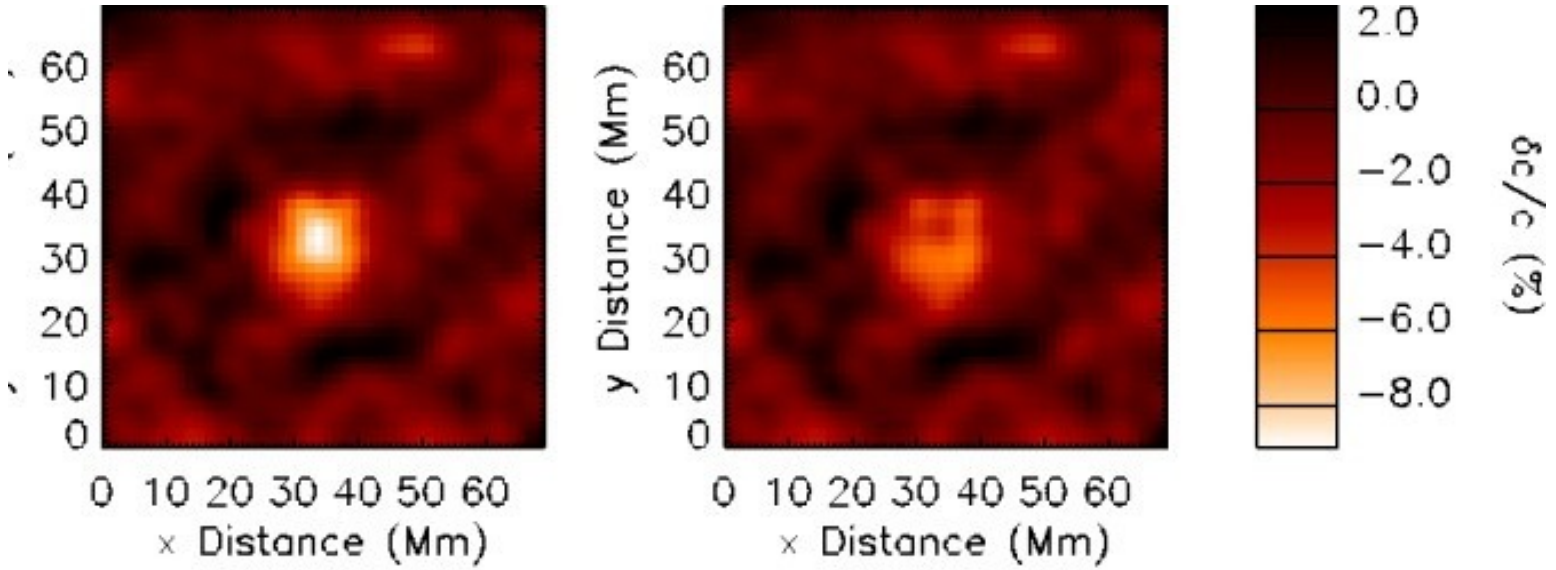

Relative sound-speed perturbation at a depth of z=-2.38 to z=-1.42 Mm with GONG data (left panel: all data, right panel: cropped data)

(From Hughes, Rajaguru, & Thompson 2005)

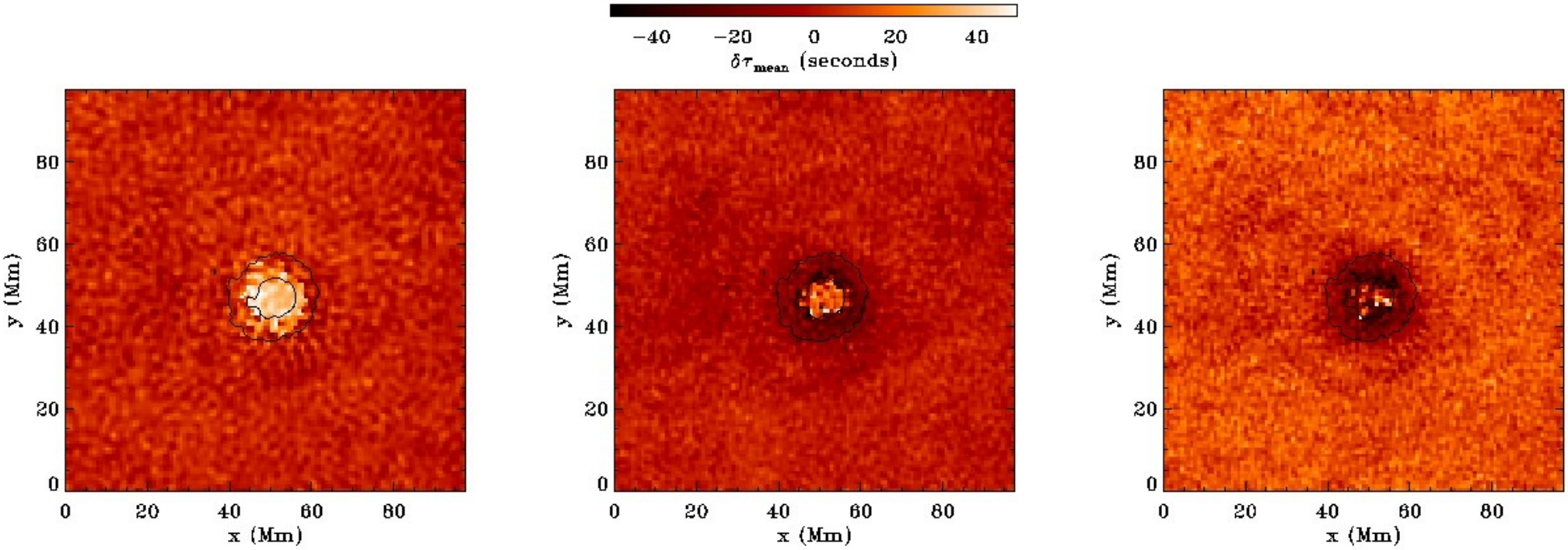

Mean travel-time perturbations in 3 different frequency bands: around 3 mHz (left panel), 4 mHz (central), and 4.5 mHz (right) for a distance of 11.6 Mm

(From Couvidat & Rajaguru 2007)

Frequency dependence of travel times

- Chou, Sun, & Chang (2000), Chou & Duvall (2000), Braun & Birch (2006) observe a frequency dependence of travel times in sunspots

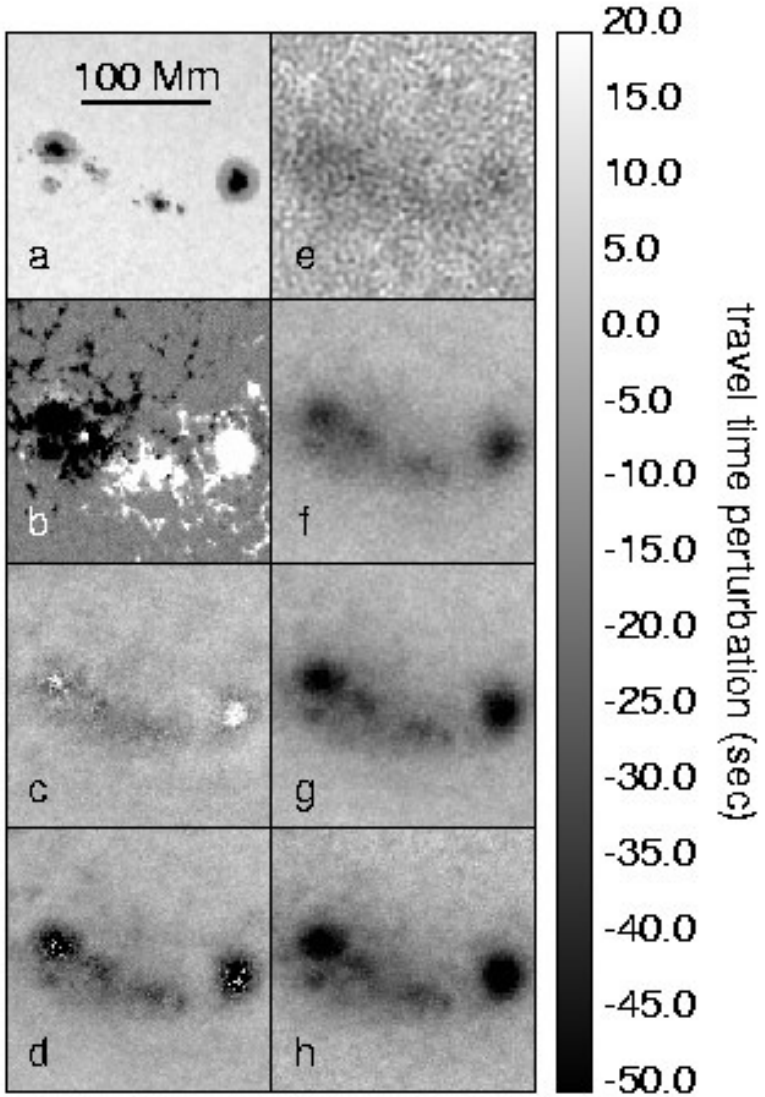

Panels (a): SOI/MDI continuum intensity; (b): line-of-sight magnetogram, (c) to (h): sample maps of the mean travel-time perturbation covering a portion of the region studied and showing sunspot group AR 9885. Panels (c) and (d) show travel-time maps for a specific phase-speed filter and a frequency filter centered at 3 and 4 mHz respectively. Panels (e) to (h) show the travel-time maps for another phase-speed filter and the frequencies 2, 3, 4, and 5 mHz respectively.

From Braun & Birch (2006)

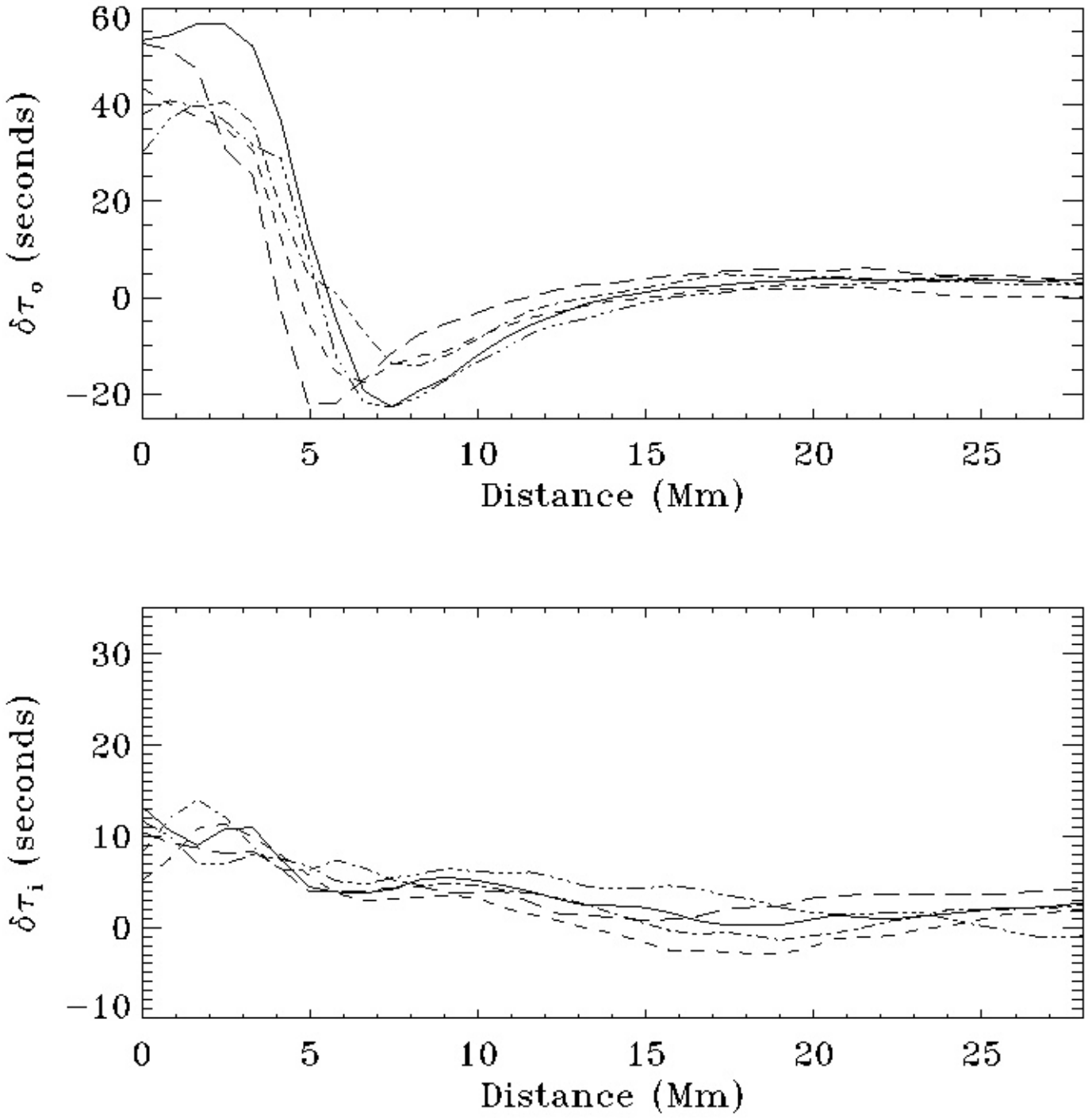

Azimuthal average of outgoing (upper panel) and ingoing (lower panel) travel time shifts for 5 sunspots and for the distance 11.6 Mm

(From Couvidat & Rajaguru 2007)

Origin of these ring-like structures ?

- Rings are mainly below penumbrae in inversion results/ inside penumbrae on travel-time maps
- Rings are only present on outgoing travel times
- Rings are very sensitive to the filtering applied to datacubes (strong frequency dependence)
- Cally (2000), Crouch & Cally (2003), Schunker et al. (2005) emphasize the effects of an inclined magnetic field on the acoustic wavefield
- Lindsey & Braun (2005) observe an anomaly in the seismic signature of sunspot penumbra (penumbral acoustic anomaly)

=> artifacts produced by interaction of surface magnetic field and acoustic waves ?

Acoustic-wave source suppression and its impact of travel times

- First mentioned by Gizon & Birch (2002): magnetic field in sunspot inhibits convection, resulting in a suppression of wave sources; this suppression is likely to affect both mean and difference travel times
- We used numerical simulations of Hanasoge et al. (2006; 2007):
  - 3D Cartesian geometry simulations of the wavefield, box of 400 x 400 x 35 Mm^3
  - Based on solar model S (from Christensen-Dalsgaard)
  - No damping
  - Absorbent boundary conditions
  - Source function prescribed such that a solar-like power spectrum is obtained

Acoustic wavefield simulation

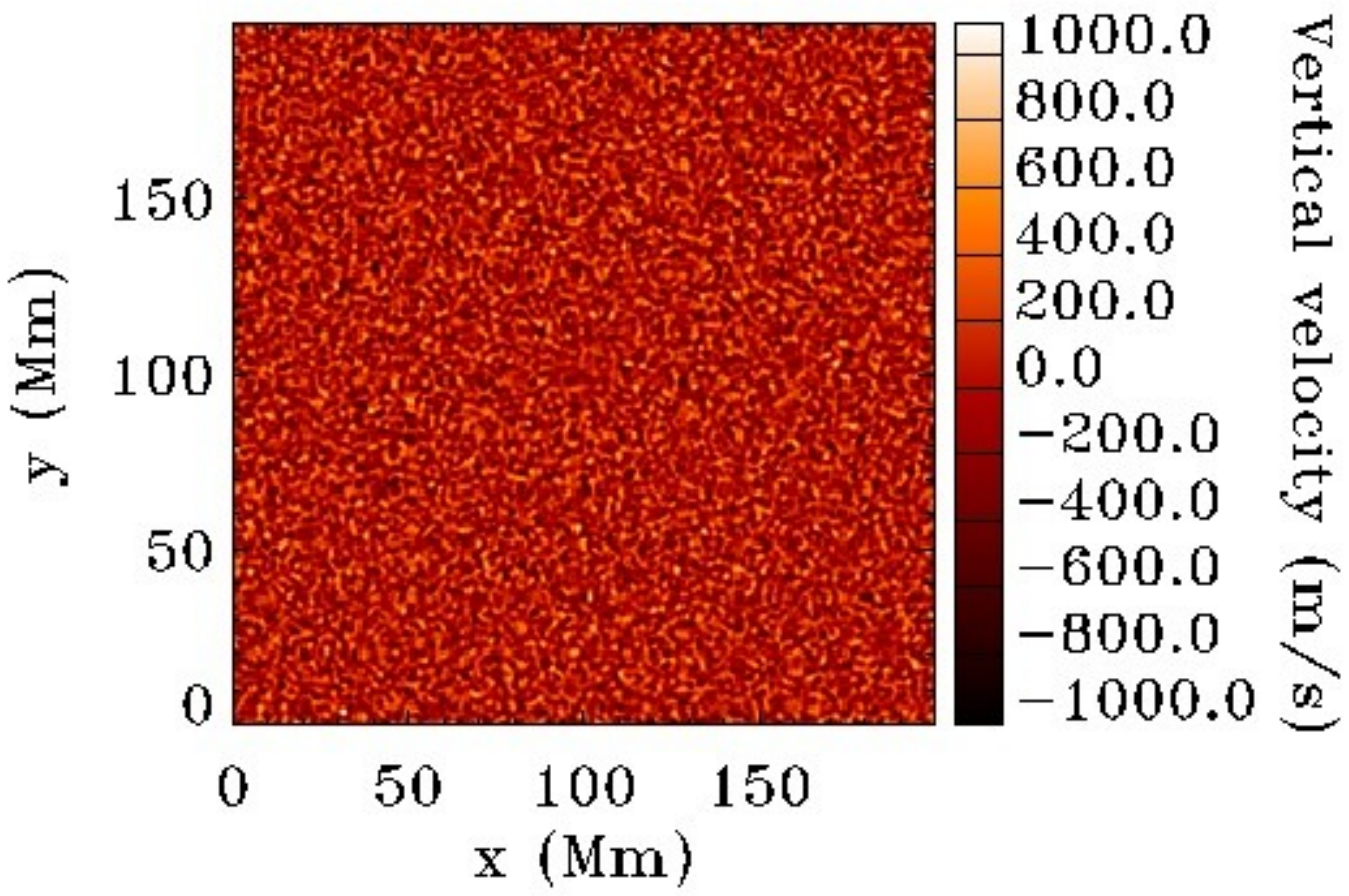

Vertical velocity at the photosphere from a numerical simulation of S. M. Hanasoge (Hanasoge et al. 2006)

Source suppression

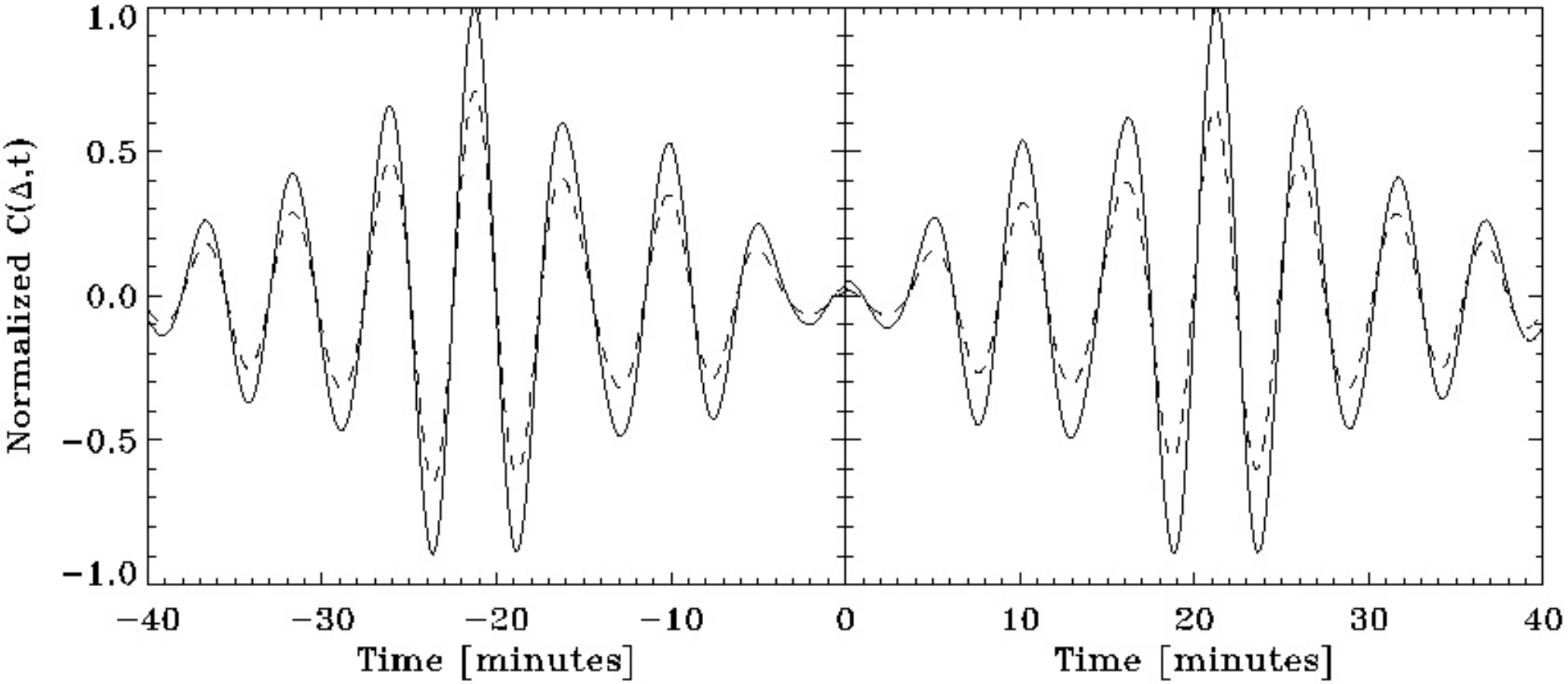

Cross-covariance centered on the first bounces for a distance of 16.95 Mm

(From Hanasoge, Couvidat, Rajaguru, & Birch, submitted)

Source suppression

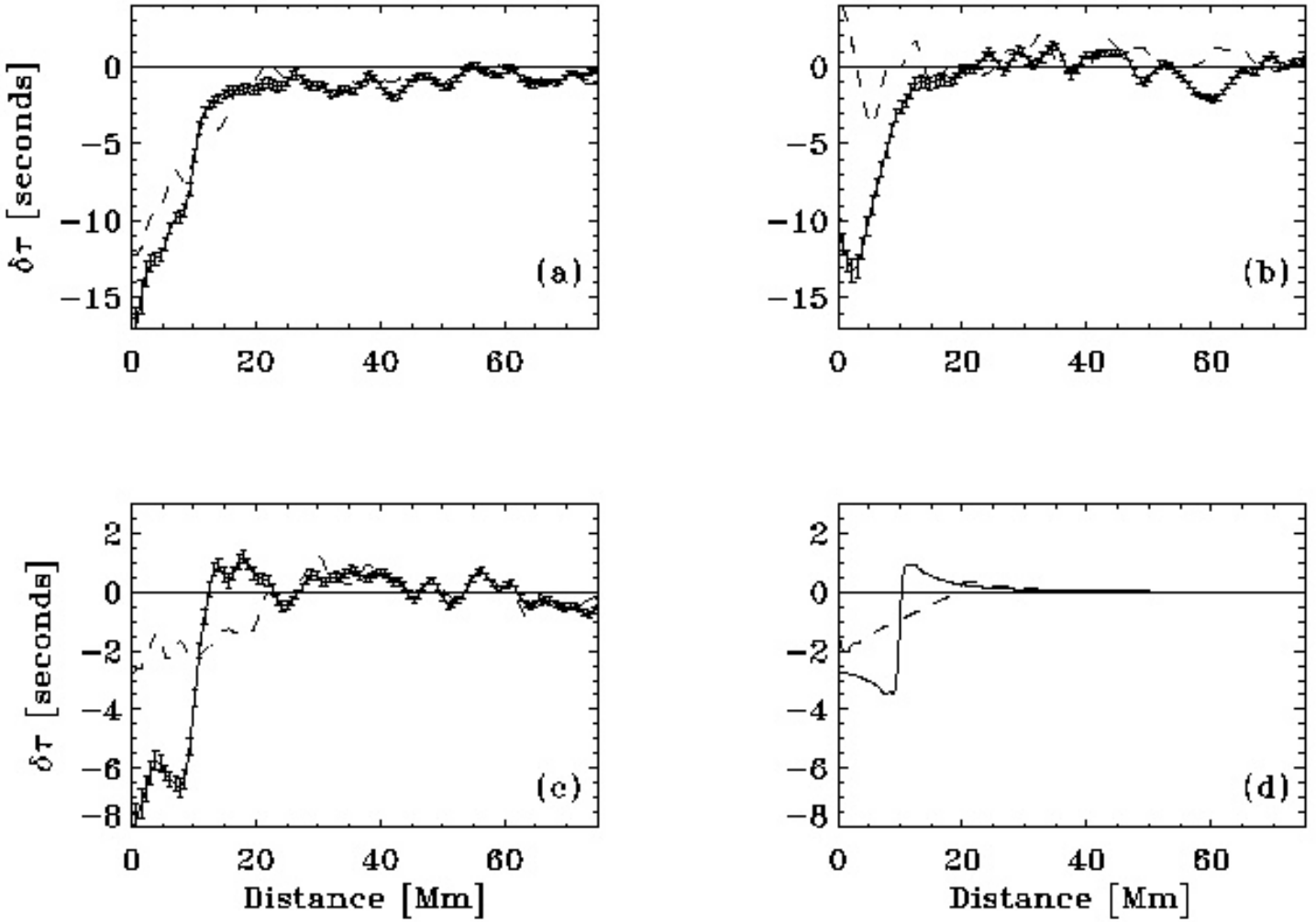

Azimuthal average of the outgoing (solid lines) and ingoing (dashed lines) travel times around the perturbation center and for a distance of a) 6.2 Mm; b) 24.35 Mm; c) 11.6 Mm and f modes; d) 10 Mm and f modes with theoretical Born-approximation kernels (from A. C. Birch)

(From Hanasoge, Couvidat, Rajaguru, & Birch, submitted)

Source suppression and inverted sound speed

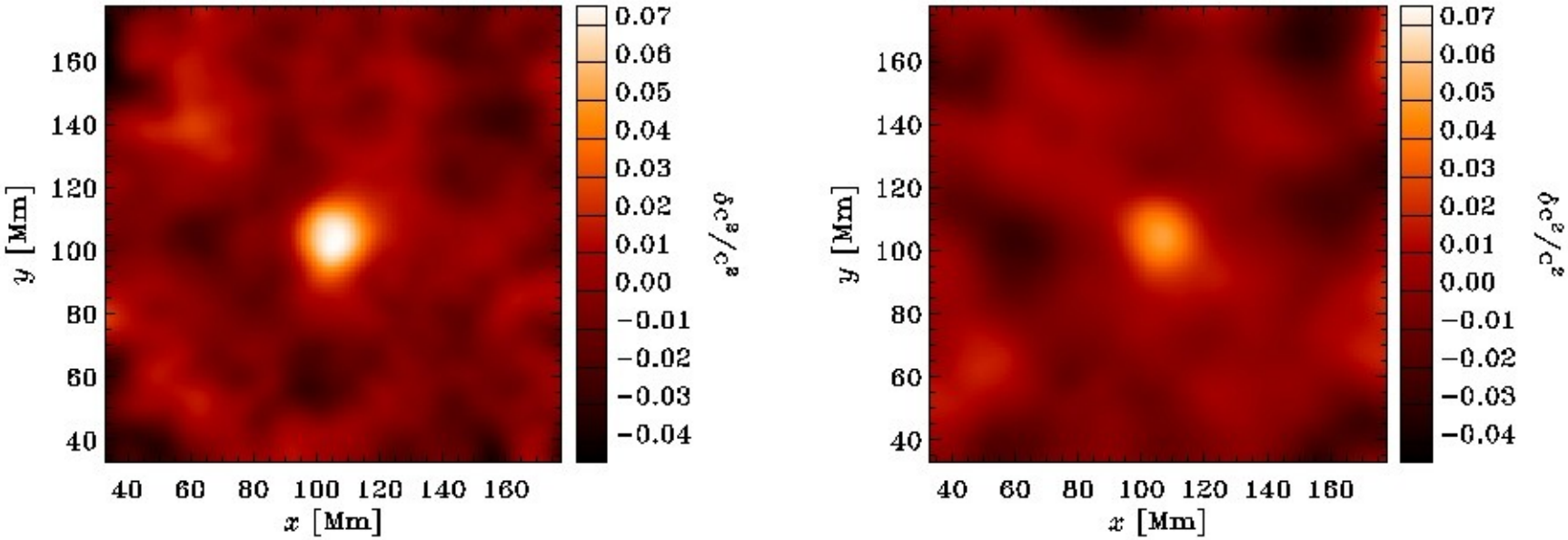

Inversion result for the noise-subtracted mean travel-time shifts. Left panel: z=-0.62 to z=0 Mm; right panel: z=-1.42 to z=-0.62 Mm

(From Hanasoge, Couvidat, Rajaguru, & Birch, submitted)

Conclusion

- Time-Distance helioseismology gives unprecedented access to solar subsurface
- Ring-like structures roughly located in the penumbra detected on the travel time maps of sunspots: likely to be due to interaction of surface magnetic field with acoustic wavefield
- Source-suppression in sunspots has significant impact on mean and difference travel times
- Magnetic field and source suppression effects (and more, see e.g. Woodard 1997) need to be taken into account when inverting for sound speed and flows below active regions
- 3D Simulations of the wavefield needed (e.g. Hanasoge et al. 2006; Cameron et al. 2007; Hartlep et al. 2007; Parchevsky & Kosovichev 2007)

Time-Distance Helioseismology (II)

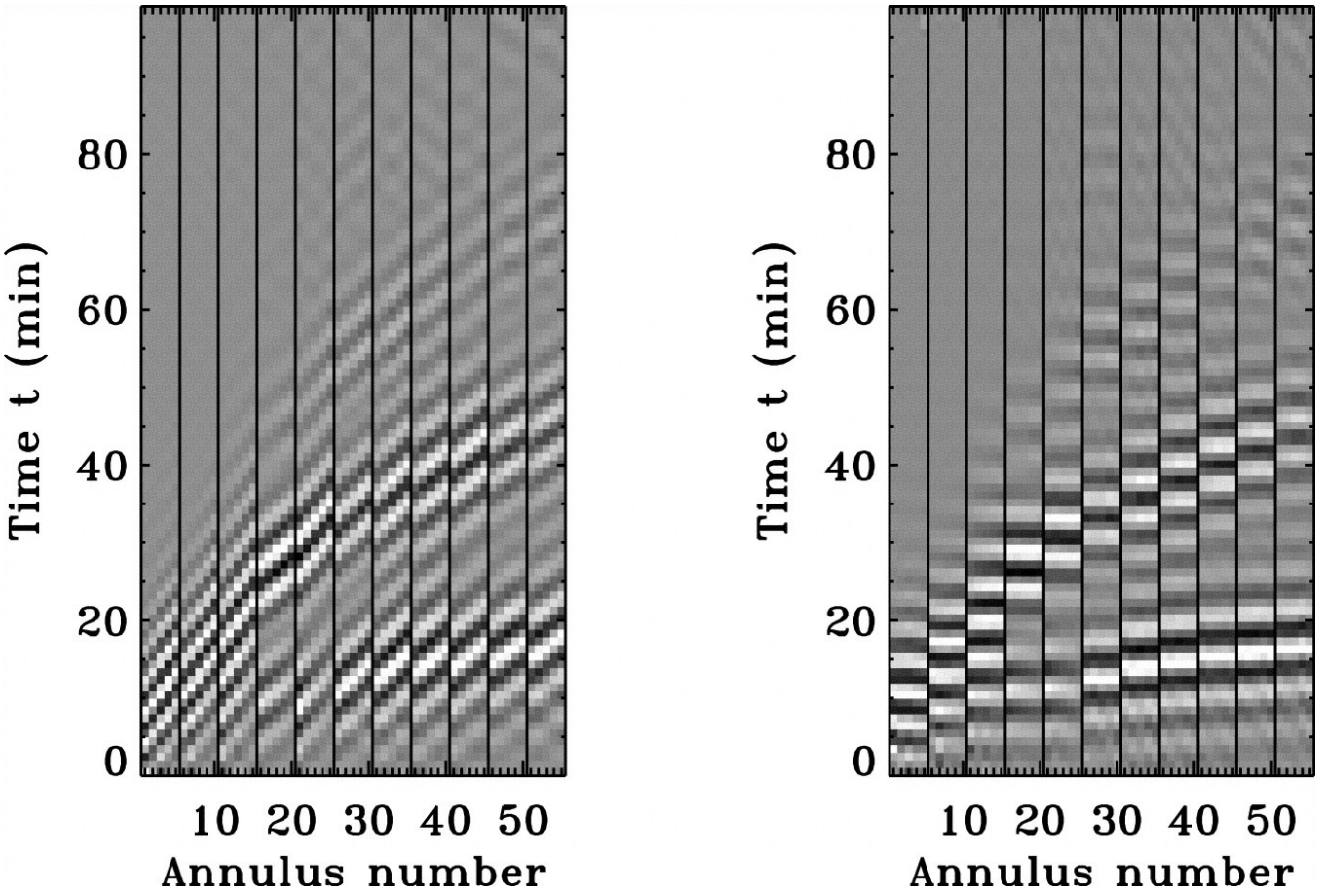

Time-distance diagram before and after shifting (from Couvidat, Birch, & Kosovichev 2006)

Flow velocity (I)

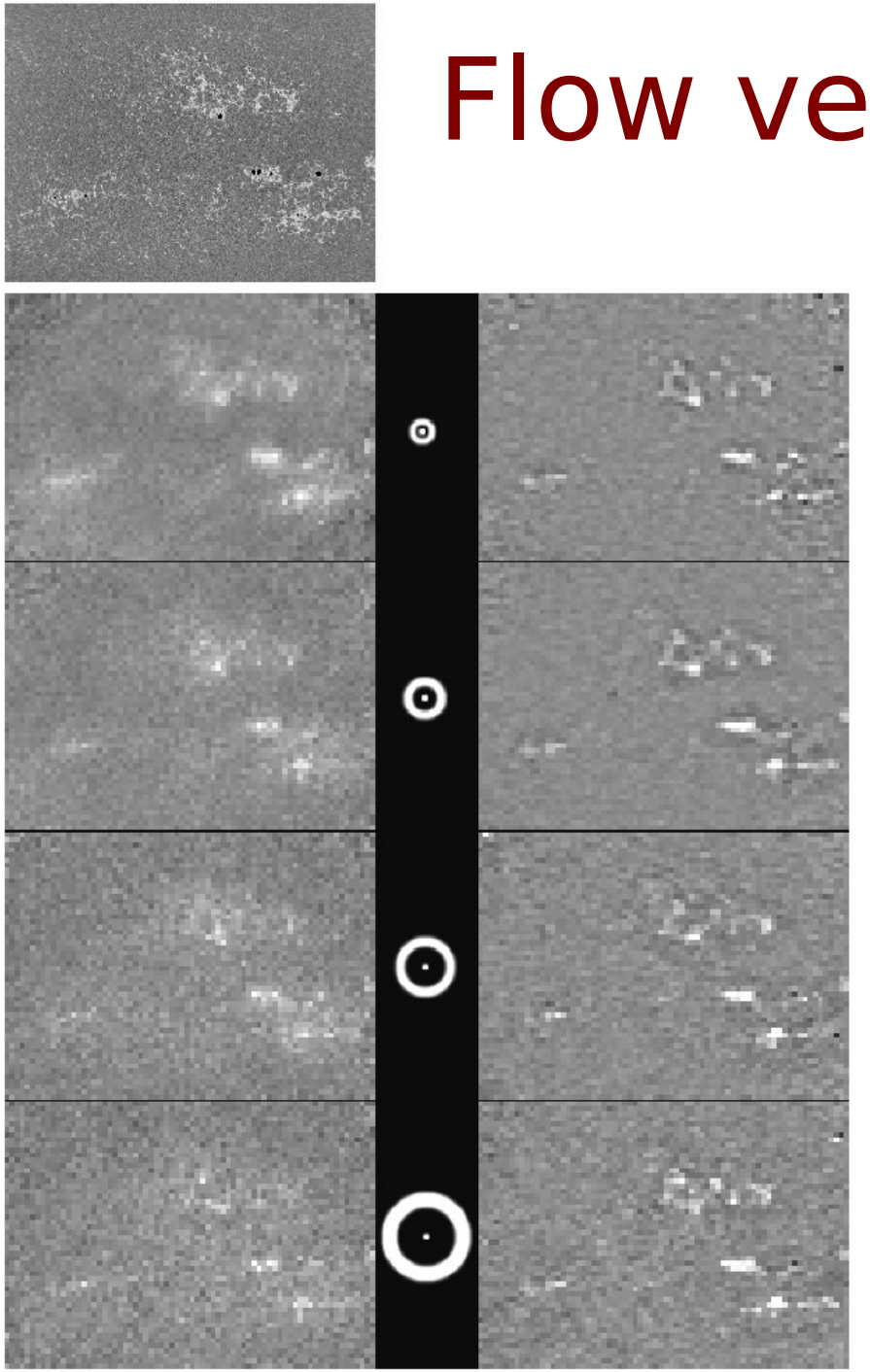

- Upper left: image of the Sun in the calcium K-line. Small dark spots are sunspots. Below are maps of the mean (left panels) and difference outgoing-minus-ingoing (right panels) travel times. The four sets of travel-time maps correspond to four different annuli, shown in the central panel. For the difference travel-time panels, white color corresponds to outgoing waves traveling faster than ingoing waves. The largest difference is about 1 minute. From Duvall et al. (1996).

Flow velocity (II)

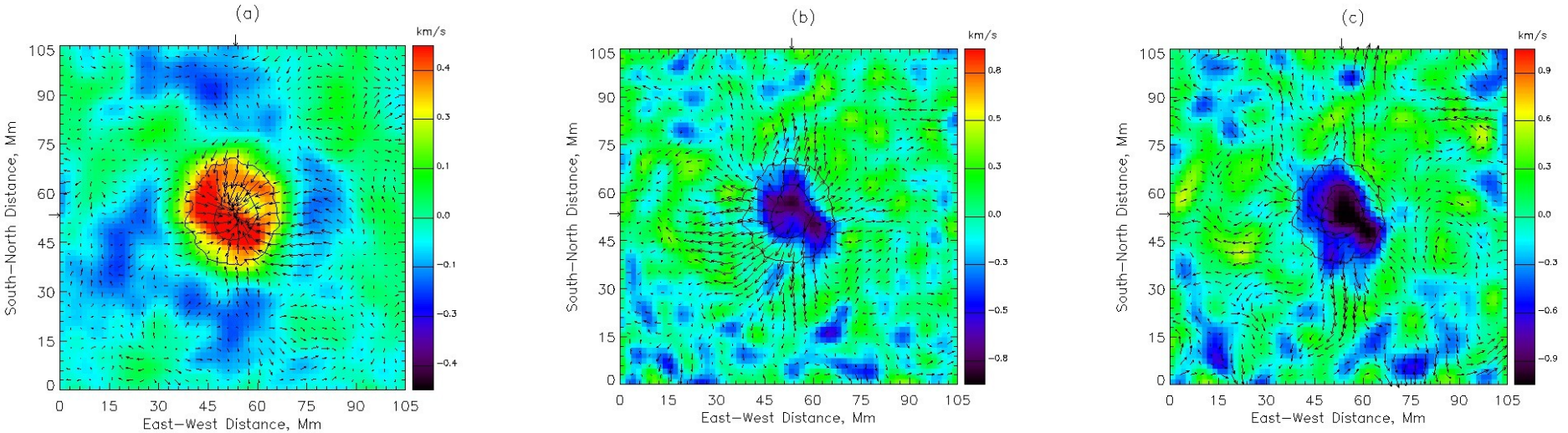

Material flows at a depth of a) 0-3 Mm, b) 6-9 Mm, and c) 9-12 Mm in and around a sunspot. Arrows show the direction and magnitude of the horizontal flows, and the background color shows the vertical flows. Positive velocity indicates downflow. The longest arrow represents 1.0 km s^{-1}. From Zhao, Kosovichev, & Duvall (2001).

Sound-speed structure

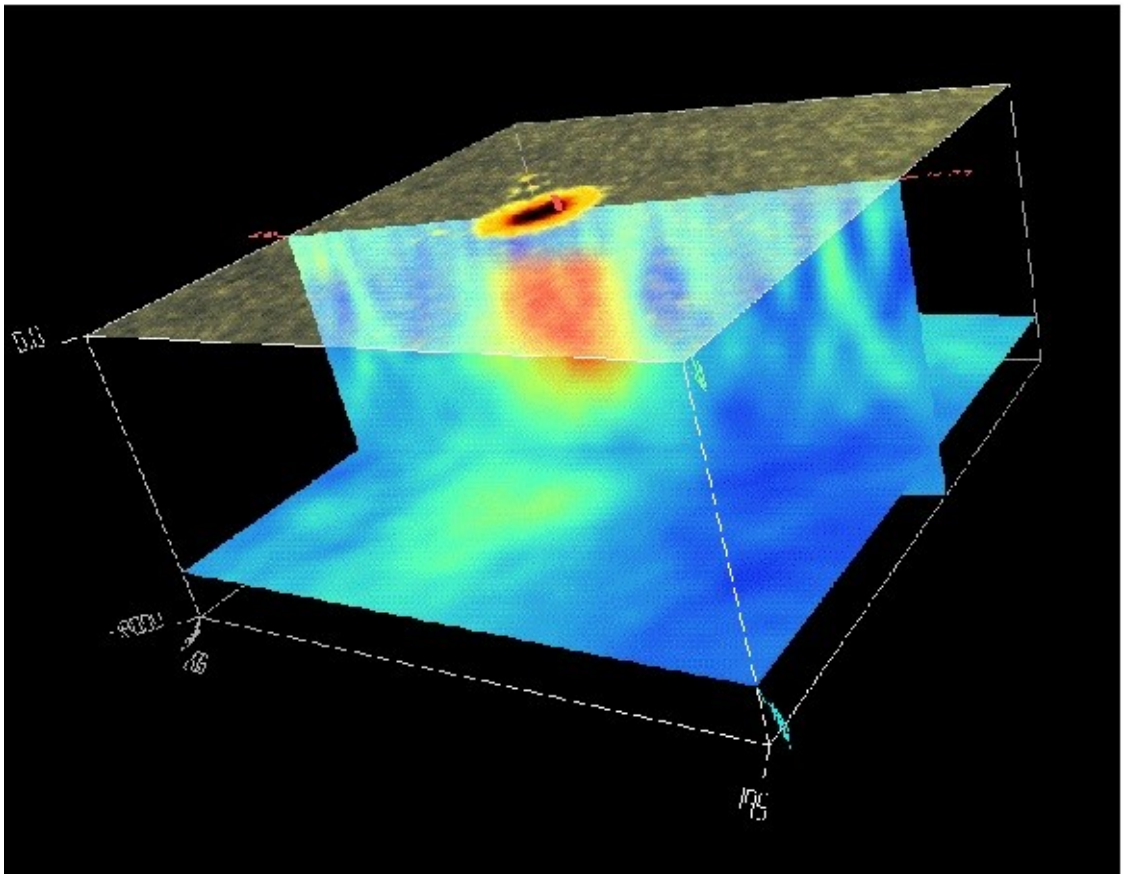

Relative sound-speed perturbation below NOAA 8243. Blue: sound-speed decrease; Red: sound-speed increase (from Kosovichev, Duvall, & Scherrer 2000)

Contamination of sunspots by surface/magnetic field effects ?

- Lindsey et al. (1996), Woodard (1997), Gizon & Birch (2002): acoustic power absorption in sunspot could explain part of the travel-time difference
- Chou, Sun, & Chang (2000), Chou & Duvall (2000), Braun & Birch (2006) observe a frequency dependence of travel times in sunspots
- Lindsey & Braun (2003) emphasize changes in acoustic wave phases when they cross magnetic field (showerglass effect)
-
- Cally (2000), Crouch & Cally (2003), Schunker et al. (2005) emphasize the effects of an inclined magnetic field on the acoustic wavefield

Mode conversion

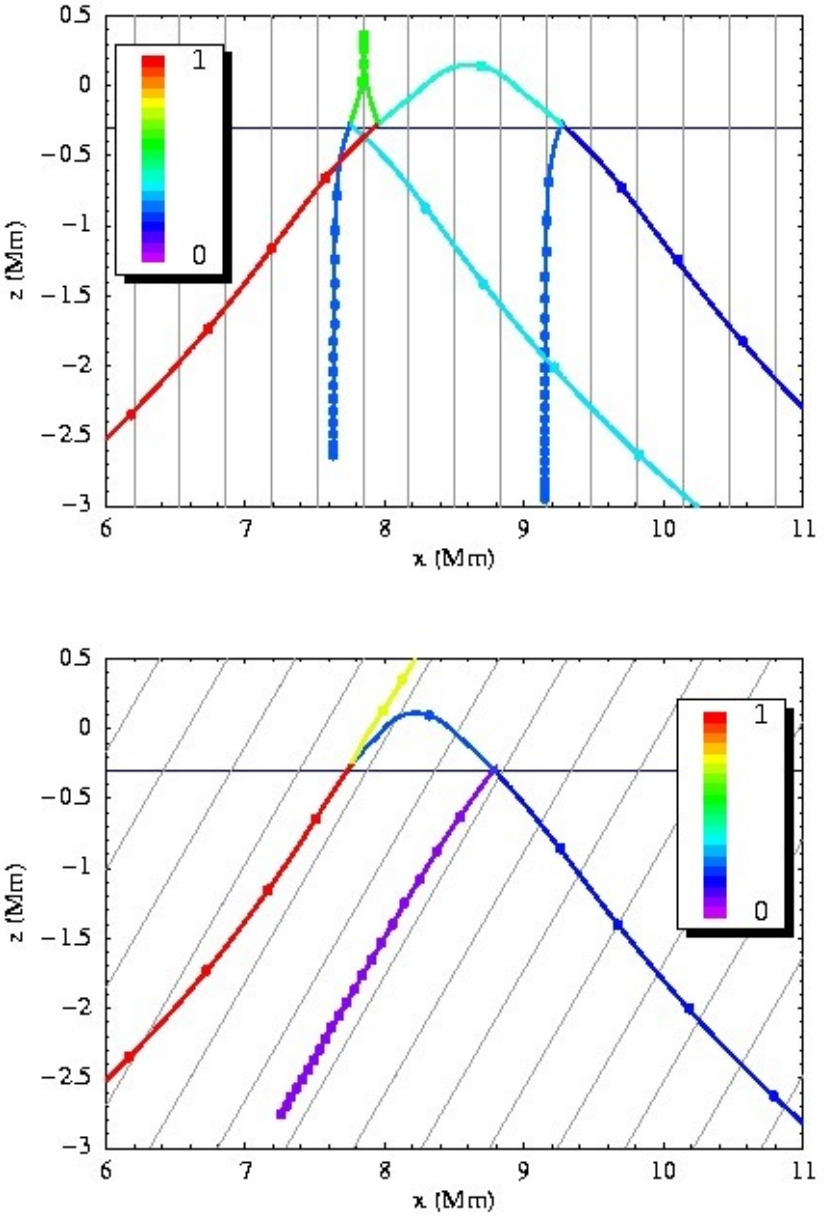

Ray-path diagrams in a vertical plane for 5 mHz acoustic waves launched horizontally from x=0 z=-5 Mm in the presence of a 2 kG magnetic field which is vertical (top panel) and inclined at 30 degrees (bottom panel). The color scale shows the percentage of energy that goes from the incoming acoustic wave (in red) to the slow acoustic mode traveling into the atmosphere and to the fast acoustic wave traveling inside the Sun. The horizontal line indicates the level at which the sound speed is equal to the Alfvén speed. The background gray lines represent the magnetic field.

From Schunker & Cally (2006)